Title

Remote spatiotemporally controlled and biologically selective permeabilization of blood-brain barrier

Authors

Xiong, Xiaobing
Sun, Yao
Sattiraju, Anirudh
et al.

Publication Date

2015-11-01

DOI

10.1016/j.jconrel.2015.08.044

Peer reviewed

Published in final edited form as:

J Control Release. 2015 November 10; 217: 113–120. doi:10.1016/j.jconrel.2015.08.044.

Remote Spatiotemporally Controlled and Biologically Selective Permeabilization of Blood-Brain Barrier

Xiaobing Xiong[1,*], **Yao Sun**[1,*], **Anirudh Sattiraju**[2], **Youngkyoo Jung**[1,2,3], **Akiva Mintz**[1,2], **Satoru Hayasaka**[1,4], and **King C.P. Li**[1]

[1]Department of Radiology, Wake Forest School of Medicine, Winston-Salem, NC 27157, USA

[2]Comprehensive Cancer Center, Brain Tumor Center of Excellence, Wake Forest School of Medicine, Winston-Salem, NC 27157, USA

[3]Department of Biomedical Engineering, Wake Forest School of Medicine, Winston-Salem, NC 27157, USA

[4]Department of Biostatistics Sciences, Wake Forest School of Medicine, Winston-Salem, NC 27157, USA

Abstract

The blood-brain barrier (BBB), comprised of brain endothelial cells with tight junctions (TJ) between them, regulates the extravasation of molecules and cells into and out of the central nervous system (CNS). Overcoming the difficulty of delivering therapeutic agents to specific regions of the brain presents a major challenge to treatment of a broad range of brain disorders. Current strategies for BBB opening are invasive, not specific, and lack precise control over the site and timing of BBB opening, which may limit their clinical translation. In the present report, we describe a novel approach based on a combination of stem cell delivery, heat-inducible gene expression and mild heating with high-intensity focused ultrasound (HIFU) under MRI guidance to remotely permeabilize BBB. The permeabilization of the BBB will be controlled with, and limited to where selected pro-inflammatory factors will be secreted secondary to HIFU activation, which is in the vicinity of the engineered stem cells and consequently both the primary and secondary disease foci. This therapeutic platform thus represents a non-invasive way for BBB opening with unprecedented spatiotemporal precision, and if properly and specifically modified, can be clinically translated to facilitate delivery of different diagnostic and therapeutic agents which can have great impact in treatment of various disease processes in the central nervous system.

Keywords

Blood-brain barrier; Stem cells; MRI; High intensity focused ultrasound; Image guided drug delivery; HSP70

Correspondence should be addressed to: King C.P. Li (kingli@wakehealth.edu).

*These authors contributed equally to this work.

Chemical compounds studied in this article: Gadopentetate dimeglumine (PubChem CID: 55466); Luciferin (PubChem CID: 5484207); Poly(lactide-co-glycolide) (PubChem CID: 23111554)

1. Introduction

The blood-brain barrier (BBB), comprised of brain endothelial cells (BECs) with tight junctions (TJ) between them, regulates the extravasation of molecules and cells into and out of the central nervous system (CNS)[1, 2]. Although the BBB serves to restrict the entry of potentially toxic substances into the CNS in its neuroprotective role, it constitutes a permeability barrier that hinders the delivery of many potentially important diagnostic and therapeutic agents to the brain[3]. Therapeutic molecules and antibodies that might otherwise be effective for diagnosis and therapy cannot cross the BBB in adequate amounts. It is believed that BBB excludes from the brain ~ 100% of large-molecule neurotherapeutics and more than 98% of all small-molecule drugs[4]. Overcoming the difficulty of delivering therapeutic agents to specific regions of the brain presents a major challenge to treatment of a broad range of brain disorders such as brain cancers, Alzheimer's disease (AD), Parkinson's disease, multiple sclerosis, and neurological manifestations of acquired immune deficiency syndrome (AIDS)[5–7].

Several strategies have been developed to modulate BBB permeability to systemically administered therapeutic drugs. The available strategies for BBB opening may be broadly classified as chemical or physical-based BBB disruptions, or drug modifications that facilitate passage through an endogenous BBB. For example, osmotic agents can temporarily shrink brain endothelial cells and loosen the tight junctions to allow hydrophilic substances to diffuse into the brain[8, 9]. Intracarotid infusion of mannitol has been clinically used to enhance chemotherapeutic drug penetration of the BBB in patients with malignant primary brain tumors or metastases[10]. Because of the technical challenges and risk of brain and ocular injury, this approach is used in only a few medical centers. The bradykinin agonist, RMP-7, has been extensively studied for increasing BBB permeability [11]. RMP-7 (combined with carboplatin) increased the delivery of carboplatin into intracranial brain tumors in mouse models[12]. However, it demonstrated unreliable curative effects for patients with glioma, and has not been approved for clinical therapy[13]. More recently, activation of adenosine receptor (AR) signaling in brain endothelial cells by adenosinergic drugs has been reported to increase BBB permeability, enabling both small and large molecules to enter the brain[14]. Physical disruption of the BBB is the oldest but most invasive method to open BBB. High-intensity focused ultrasound (HIFU) with or without microbubbles has been developed to use mechanical effects to disrupt the BBB[15–19]. Drug modification has also been extensively studied to increase BBB entry. To achieve this goal, drug molecules can be modified to be more lipophilic to increase the likelihood of BBB penetration[20], or can be packaged in a vector that crosses the BBB by receptor-mediated endocytosis[21]. However, drug modification is limited by chemical properties of individual drugs or receptor expression on endothelial cells in BBB.

Given the lack of a universally successful method of penetrating the BBB to deliver therapeutics, there is a great need to develop a translatable method which allows precise spatiotemporal control down to microscopic level to facilitate the entry of drugs across the BBB for treatment of neurological diseases. Recent reports have demonstrated remote activation of engineered cells *in vivo* by light[22–24], radio waves[22] or ultrasound[25] using inducible promoters to control transgene expression. Among them, spatial and

temporal control of gene expression has been made through the use of local heat deposition via focused ultrasound coupled with the use of thermosensitive promoter[25–27]. A recent study also demonstrated the feasibility to locally activate *in vivo* transgene expression of genetically engineered cells by focused ultrasound under MR-guidance (MR-HIFU)[25, 26]. Furthermore, transcranial magnetic resonance-guided focused ultrasound (tcMRgFUS) technology has been used in clinical trial for the non-invasive treatment of various brain disorders such as essential tremor, and neuropathic pain proving that it is clinically possible to precisely deliver heat to target areas of the brain non-invasively[28–30].

Due to their capacity to migrate to disease sites, stem cells are emerging as feasible vehicles to therapeutically target different diseases in the central nervous systems and other sites[31–34]. One major challenge that limits the translational potential of stem cells as therapeutic vehicles is the fact that in addition to migrating towards the targeted diseased sites, stem cells are also attracted towards normal areas in the body that may be harmed if the stem cells non-selectively deliver or express highly toxic therapies[35].

We propose to use a combination of stem cell delivery, heat-inducible gene expression and mild heating with HIFU to remotely permeabilize BBB with unprecedented spatiotemporal precision. We propose to administer stem cells engineered to express pro-inflammatory factors that will permeabilize the BBB but only trigger their expression after heating with non-invasive image-guided HIFU. With this approach, the permeabilization of the BBB will be limited to where selected pro-inflammatory factors will be secreted secondary to HIFU activation, which is in the vicinity of the engineered stem cells and consequently both the primary and secondary disease foci. If successful, this degree of spatial and temporal precision in BBB permeabilization will be unprecedented. Our proposed approach can potentially be used as a remote controlled spatiotemporally precise platform technology for selectively permeabilizing the BBB which can be used to facilitate diagnosis and treatment of many CNS diseases.

2. Materials and methods

2.1. Animals

8-week old adult male athymic nude rats (~ 240 g, Harlan, Indianapolis, IN, USA) were used. All animal experiments were performed in compliance with the Institutional Animal Care and Use Committee (IACUC) at the Wake Forest University School of Medicine.

2.2. Lentiviral plasmids

The 400 bp minimal human HSP70B promoter was a kind gift from Dr. Chrit Moonen of Université Victor Ségalen, France[27]. The heat-inducible gene expression system was custom made from lentivrial plasmids by Gentarget (San Diego, CA). The lentivrial plasmid containing a rous sarcoma virus promoter (RSV) and dual fusion marker RFP-Blasticidin, was used as the backbone for cloning. The HSP70 sequence was ligated into the lentiviral plasmid, and the green fluorescence protein (GFP) or human TNFα codon sequence were cloned under HSP70 promoter to produce heat-inducible plasmids (Fig. 1A). The sequence verified constructs were packaged as lentiviral vectors in HEK293-TLV cells by using

lentiviral packaging plasmids. The produced lentivector has a titer around 1 ×10^7 IFU/ml measured by ELISA assay.

2.3. Cell culture and in vitro studies

Human bone marrow mesenchymal stem cells (MSCs, Lonza, Walkersville, MD) were cultured in Dulbecco's modified Eagle's medium (DMEM) supplemented with 10% fetal bovine serum (FBS). Jurkat cells and B16F10 cells were cultured in RPMI1640 medium supplemented with 10% FBS. Mouse neuron stem cells (NSCs) were cultured in the NeuroCult™ NS-A proliferation medium according to manufactuer's instruction (Stemcell Technologies Inc., Vancouver, Canada).

For gene transduction, 20 μl of lentiviral particles (mixed with polybrene at a 1:1 ratio) were placed in the media of cells in a 24-well plate and centrifuged (1200 RPM at 32°C) for 60 minutes and subsequently placed overnight under normal cell culture conditions (37°C/5% CO_2). After 24 h, the medium was replaced and cells were incubated at 37°C for a further 48 h. Stable transfected cells were selected with 100 μg/ml blasticidin. For validation and optimization of heat-induced gene expression in vitro, stable transfected cells placed in Eppendorf tubes were precisely heated at 37°C–45°C and for different durations using a PCR cycler. The cells were then placed in 24-well plate in 6 replicates and incubated at 37°C in a 5% CO_2 incubator for recovery. Luciferase activity was measured 14 h after heating induction by adding D-luciferin using a microplate reader (Biotek Instruments, USA). Bioluminescence imaging was also performed using taken using a Xenogen IVIS 100 imaging system. To validate TNFα expression after heat induction, MSCs engineered with HSP70(F-Luc-2A-TNFα) were induced at 43°C for up to 20 minutes and incubated at 37°C for 14 h. Cell culture supernatants were collected, centrifuged for 10 min at 3000 g to remove floating cells and debris, and stored at −80°C. Supernatants were analyzed for TNFα by ELISA using a human TNFα ELISA kit according to the manufacturer's instructions (Thermo Scientific, IL, USA). The plates were read on a plate reader (Biotek Instruments, USA) at 450 nm (reference filter 550 nm) within 30 minutes. The luciferase activity was measured after adding D-luciferin. The minimum detectable concentration of TNFα was 2.0 pg/ml.

2.4. Intracranial stem cell implantation

Rats were anesthetized with an i.p. injection of ketamine (50 mg/ml) and xylazine (2.6 mg/ml), and placed in a small animal stereotaxic apparatus affixed with a microinjector unit (Harvard Apparatus, Holliston, MA). A 1-cm-long midline incision was made in the scalp, beginning midway between the eyes and terminating behind the lambda. A 3 mm burr hole was created with a surgical drill (Harvard Apparatus, Holliston, MA) 1.5–2 mm right of the midline and 0.5–1 mm posterior to the coronal suture through the scalp incision. For stem cell injections, a 10 μl syringe (Hamilton Co., Reno, NV) with a 30-gauge needle was mounted onto the injection pump and the needle positioned directly over the bregma. The x, y, and z axis coordinates were all set to zero. The needle was then positioned at the entry point, 0.5 mm posterior and 3.0 mm lateral of the bregma to the right. The needle was slowly inserted into the right ventricle to a depth of 4 mm below the surface of the skull, and the MSCs (1.0 × 10^6 cells in 5 μL of PBS) were injected at a rate of 1μl/min. The needle was

left in place for 4 min and then retracted at a rate of 1 mm/min to prevent the reflux of stem cells. Incisions was sutured following tumor cell implantation (Suture: Suture with Needle Prolene™ Polypropylene, Monofilament Size 6-0 18 Inch Blue P-1 Nonabsorbable; Pattern-standard pattern-stitches are placed on the surface using the above suture material). Following surgery, ketoprofen (5 mg/kg) was subcutaneously administered every 8 hours for the first 2–3 days following surgery.

2.5. Bioluminescence image acquisition and analysis

Bioluminescence imaging was performed with a highly sensitive, cooled charge coupled device camera mounted in a light-tight specimen box (IVIS 100 imaging system, Xenogen, USA). To validate HIFU-induced gene expression in vivo, MSCs-HSP70(F-Luc-2A-GFP) were stereotactically implanted into the brains of athymic nude rats (1×10^6 cells per rat). Gene expression was induced by MRI-guided HIFU for 15 minutes. 8 and 48 hours after HIFU induction, rats were injected intraperitoneally with the substrate D-luciferin (150 mg/kg in phosphate-buffered saline) and anesthetized with isofluorane (1–3%). Bioluminescence imaging (BLI) was also performed using taken using a Xenogen IVIS 100 imaging system. The anesthetized rats were placed onto a warmed stage inside the light-tight camera box with continuous exposure to isofluorane (1–2%). The data acquisition time was 60s. The low levels of light emitted from the bioluminescent regions were detected using an IVIS camera system, integrated, digitized and displayed. Regions of interest (ROIs) from displayed images were defined, analyzed and processed using Living Image software (Caliper Life Sciences).

2.6. HIFU treatment

The HIFU treatment was conducted with a customized MRI/MR thermometry-guided preclinical HIFU unit (RK-100, FUS Instruments Inc., Toronto, Ontario, Canada) to deliver ultrasound energy to the rat brain for pHSP70 induction. The system can deliver ultrasound exposures ranging from high-power continuous sonications (thermal coagulation) to pulsed sonications for applications such as transcranial therapy, drug delivery and activation. The system probe is a spherically focused ultrasound transducer with a center frequency of 1MHz and a focal spot size around 1–2mm in diameter and 5–6mm in length. The probe is mounted on a MR-compatible computer-controlled three-axis positioner to allow for precisely focusing on the targeted site. The probe is immersed in a tank full of degassed and deionized water for acoustic coupling. Prior to the HIFU treatment, the focal spot is registered with the MR coordinates with a method already established[15]. During treatment, the focused spot was placed against the rat right superior cranium (site of the stem cell injection) on the bed of the Siemens Skyra 3T scanner. The rat was rest supine in a degassed and deionized water disk on a gel pad with ultrasound transparent film on the bottom. Continuous ultrasound exposure (0.9W) was performed to the rat brain to heat the targeted site to approximately 43°C, a temperature that is non-toxic to brain tissue but induces genes expression under the HSP70 promoter. The acoustic intensity around the focused spot and the HIFU induced temperature change is controlled and monitored in near real-time by using MR-thermometry. The HIFU output power might be tuned a little bit based on the temperature feedback from MR thermometry to reach and maintain around the desired temperature during the treatment.

2.7. MRI and MR Thermometry

The MRI scans were conducted with a customized surface coil (RK-100, FUS Instruments Inc., Toronto, Ontario, Canada) attached to a 3T Siemens Skyra scanner (Siemens AG, Erlangen, Germany) to provide image guidance, temperature monitoring, and visualization of enhanced BBB permeabilization after HIFU treatment. Image guidance was based on T2-weighted images acquired by MRI using 3D dual echo steady-state sequences (echo time (TE)/repetition time (TR)= 5.7/17ms, 10cm field of view (FOV), 256 × 256 matrix size, 88 slices, 0.39×0.39 mm^2 in-plane resolution, 0.4mm slice thickness, and 5 min. scan time). The temperature monitoring was performed based on MR thermometry using a 2D gradient echo sequence[36](baseline temperature: 37.2°C, TE/TR=8.7/30ms, 10cm FOV, 128 × 128 matrix, 5 slices, 6/8 partial Fourier factor, 0.78 × 0.78mm^2 in-plane resolution, 2.5 mm slice thickness, and 14.5 s temporal resolution). A reference phase image was acquired prior to HIFU treatment and the temperature was estimated by calculating the phase difference between the present phase during heating and the reference phase in the treatment area. Another area outside the treatment area was also chosen to correct the magnetic field drift during the HIFU treatment. The temperature maps covering the treatment area were updated and monitored in every time frame (14.5 sec). Contrast-enhanced T1-weighted MRI images were acquired using a spoiled gradient echo sequences (TE/TR=6/13.5ms, 10cm FOV, 256 × 256 matrix size, 104 slices, 0.39mm in-plane resolution, 0.4mm slice thickness, and 6min scan time) to verify the change of BBB permeability in the treated site after HIFU treatment. A gadolinium-based MRI contrast agent, Magnevist (Gd-DTPA; 0.125 mmol/kg), which has been commonly used in previous studies to verify the permeability of brain through blood-brain barrier [15], was injected via tail vein in order to detect a region where brain permeability was changed.

2.8. Cryosectioning of frozen brain tissue for fluorescence microscopy

After confirmation of BBB opening by contrast-enhanced T1-weighted MRI image, a mixture of fluorescent PLGA nanoparticles (Phosphorex, Inc., MA) with different sizes was intravenously injected via tail vein 2 days after HIFU induction. The PLGA nanoparticles with average diameter at 100 nm are labeled as red (652/668 nm, Ex/Em) and the PLGA nanoparticles with average diameter at 300 nm are labeled as green (445/500 nm, Ex/Em). 24 hours after systemic nanoparticle injection, rats were euthanized and perfused with saline. The brain was removed and frozen in OCT embedding medium (Sakura, Torrance, CA, USA) at −80°C. Before sectioning the frozen tissue, brain tissue blocks were transferred to a cryotome cryostat (e.g., −20°C) and allowed to equilibrate to the temperature of the instrument. The tissue sections (10 μm thickness) were placed on poly-L-lysine-coated glass slides. Frozen sections of thickness were prepared with a cryotome and immediately examined under the fluorescence microscope.

2.9. Statistical analysis

In vitro experiment was performed three to five times and the data are plotted as mean values ± standard error of means. For performing in vivo experiments, rats were assigned into different groups without any bias and each group consisted of four to six rats. Two-sample t-test was used to statistically analyze the gene expression (MSCs-HSP70(F-Luc-2A-

GFP)) between the animals treated by HIFU (N=4) and those that were not treated by HIFU (N=4). The *in vivo* data of MRI guided HIFU induced BBB opening by MSCs with TNFα expression were statistically analyzed in the region of interest by a one-way ANOVA between the HIFU-treated animals (N=6) and the two control groups, namely HSP70-F-Luc-TNFα without HIFU treatment (N=4) and the HSP70-F-Luc-GFP with HIFU treatment (N=4). The statistical significance was calculated by the Tukey's method. Data were expressed as mean ± SEM, and difference were considered significant at $p < 0.05$.

3. RESULTS

3.1. In vitro validation and optimization of heat-induced gene expression

To demonstrate heat-activated gene expression, we first constructed a lentiviral plasmid expression system for heat-activated gene expression and optimized the gene expression using different cell lines. The lentiviral plasmid construct (pLenti-HSP70(F-Luc-2A-GFP)-RSV(RFP-BSD)) consists of the heat-inducible HSP70 promoter driving expression of firefly luciferase (F-Luc) and green fluorescence protein (GFP), and the RSV promoter driving expression of two screening markers: red fluorescent protein (RFP) and blasticidin selection marker (BSD) (Fig. 1A). The construct was packaged into lentiviral particles and transduced into human mesenchymal stem cells (MSCs) as indicated by the red fluorescence (Fig. 1B). To validate heat-induced gene expression, we heated the engineered MSCs (MSCs-HSP70-(F-Luc-2A-GFP)) at 43 °C for 20 minutes. The heat-induced MSCs demonstrated obvious green GFP fluorescence as compared to the non-heated controls (Fig. 1B). To optimize the induction temperature and duration of time, we heated MSCs at different temperatures (between 42 and 45°C) for different lengths of time, and measured the luciferase activity. As expected, luciferase activity of MSCs-HSP70(F-Luc-2A-GFP) was tightly dependent on temperature and induction time. Induction at 43°C for 15 minutes produced a peak of 16-fold increase in luciferase activity compared to the control incubated at 37 °C (Fig. 1C). Heat-induced gene expression system of pLenti-HSP70(F-Luc-2A-GFP)-RSV(RFP-BSD) was also validated with other cell lines. We transduced the heat-inducible construct into different cells (Jurkat cells, B16F10 cells, and mouse neuron stem cells (NSC)) and tested their heat-induced gene expressions (Supplementary Fig. 1). At 37°C, the control temperature, luciferase activity in all the cell lines was at background levels, while heat induction between 42°C–44°C led to significant luciferase activity increase to various extent which was dependent on induction time. All cell lines demonstrated a peak bioluminescence signal within a period of induction time. However, there was a large discrepancy in the magnitude of luciferase activity and peak induction time between cell lines. For example, the highest luciferase activity was seen with Jurkat cells and B16F10 cells for 30 minutes and 40 minutes of heat induction time (Supplementary Fig. 1A and 1B), while 15 minutes of heat induction led to peak luciferase activity for MSCs (Fig. 1C). Compared with the baseline levels at 37°C, peak luciferase activity was 8-folds for Jurkat cells, 28-folds for B16F10 cells, and 6-folds for NSCs cells at 43°C heating. The heat inducible gene expression was also confirmed by fluorescence microscopic observation; all the cell lines with HSP70-driven GFP demonstrated strong green fluorescence after heat induction (Supplementary Fig. 1).

3.2. In vivo validation of MRI-guided HIFU induced gene expression by MSCs after intracranial implantation

We tested the gene expression efficiency of engineered MSCs induced by MRI-guided HIFU after intracranial implantation. We stereotactically implanted engineered MSCs 4.0 mm deep into the right frontal lobe of athymic nude rats through a burr hole. 3 days after implantation, the rats were placed supine onto the HIFU device which is in a 3Tesla Siemens Skyra MRI scanner. The MSCs location was identified with T2-weighted MRI images obtained with a 3D dual-echo steady-state sequence and was used to guide the HIFU treatment (Fig. 2A, **upper left panel**). HIFU was focused on the MSCs location through acoustic coupling media and the intracranial temperature was monitored in near real-time using MR thermometry to allow for feedback controlling of the HIFU treatment (Fig. 2A, **upper right panel**). As expected, HIFU treatment led to robust F-Luc expression, in contrast to the control that had the same number of MSCs cells with reported construct but was not heated by HIFU (Fig. 2B). Quantification of bioluminescence signal in regions of interest at 8 and 48 h after HIFU treatment revealed 38-fold and 25-fold increase in bioluminescence signal intensity compared to the untreated controls (Fig. 2C). This result is consistent with the in *vitro* findings and demonstrates that MRI-guided HIFU is capable of inducing gene expression of engineered MSCs after intracranial implantation.

3.3. MRI-guided HIFU treatment for BBB opening by MSCs with inducible TNFα expression

Following the validation of MRI-guided HIFU induced gene expression by MSCs, we replaced the heat-inducible GFP reporter gene with TNFα sequence to construct heat-inducible TNFα expression system (pLenti-HSP70(F-Luc-2A-TNFα)-RSV(RFP-BSD)) (Fig. 3A). The construct was packaged in lentiviral particles and successfully transduced into MSCs as indicated by the red GFP fluorescence (Fig. 3B). The engineered MSCs were heated in a PCR thermal cycler. After heat induction, the luciferase activity of the engineered MSCs was measured by bioluminescence imaging and the TNFα expression was detected by ELISA. We detected strong luciferase activity for MSCs-HSP70(F-Luc-2A-TNFα) (Fig 3C), and Elisa measurement revealed a high TNFα level (up to 700 ng/ml) in the cell supernatant after induction at 43° for 10 min, indicating the induced MSCs robustly expressed secretable TNFα (Fig 3D).

Next, we intracranially implanted the MSCs-HSP70(F-Luc-2A-TNFα) into the right frontal lobe of athymic nude rats. 3 days after implantation, HIFU was applied under MRI guidance and temperature was monitored in near real-time by MR thermometry (Fig. 4A). 1 day after HIFU induction, rats were imaged for bioluminescence (BLI) after being anesthetized and injected i.p. with D-luciferin. We detected strong luciferase activity in rat brains implanted with MSCs-HSP70(F-Luc-2A-TNFα) or MSCs-HSP70(F-Luc-2A-GFP) treated by HIFU, while rats implanted with MSCs-HSP70(F-Luc-2A-TNFα) without HIFU treatment showed background luciferase activity (Fig. 4B), indicating successful gene expression by HIFU induction. Contrast-enhanced T1-weighted MRI images were acquired 2 days after HIFU treatment to verify the change of BBB permeability in the treated site. Small molecule Magnevist (Gd-DTPA; 0.125 mmol/kg) was used as the contrast agent for brain permeability and injected into the rats by tail vein. Enhancement was observed in the targeted regions of the rat brain implanted with MSCs-HSP70(F-Luc-2A-TNFα) construct

and treated with HIFU. In contrast, rats implanted with MSCs-HSP70(F-Luc-2A-TNFα) without HIFU treatment and rats implanted with MSCs-HSP70(F-Luc-2A-GFP) with HIFU treatment did not demonstrate significant contrast enhancement on T1-weighted images (Fig. 4C). Analysis of the T1-weighted images revealed a 3-fold contrast-enhancement in the target regions compared to the controls (Fig. 4D, and Supplementary Fig. 2). After confirming BBB opening by contrast enhanced T1-weighted MRI images, a mixture of fluorescent poly(lactic-co-glycolic acid) (PLGA) nanoparticles with different sizes corresponding to different fluorescent labels were administered intravenously into the rats 2 days after HIFU induction. The frozen sections were prepared and immediately examined under the fluorescence microscope. We observed that both red fluorescence and green fluorescence (Fig. 4E) extravagated into the brain, indicating that that both 100nm and 300nm PLGA nanoparticles successfully crossed the BBB after HIFU induced TNFα production by MSCs and penetrated to the brain tissue at the HIFU-exposed MSCs. As expected, we didn't find obvious nanoparticle accumulation in brain for control groups.

Discussion

In this study we have provided evidences that a combination of stem cell delivery, heat-inducible gene expression and mild heating with MRI guided HIFU can be used to remotely permeabilize BBB with high spatiotemporal precision and biologic selectivity. We demonstrated that MR-thermometry enabled HIFU can be safely used to intracranially heat the implanted engineered MSCs and induce transient TNFα expression, leading to focal BBB permeabilization allowing for penetration of small molecular MRI contrast agent (Magnevist) and up to 300 nm size nanoparticles of PLGA into the brain. A major advantage of this approach over using HIFU with or without microbubbles for BBB permeabilization is the fact that our approach relies on the combination of physical energy deposition and a subsequent biologic response. As a result even though a much larger volume of the brain will be mildly heated by HIFU, the BBB permeabilization will be much more focused and occurred only where the activated engineered stem cells are located. Another advantage of our proposed approach is that there is no need to have *a priori* knowledge of where the disease foci are in determining the volume for HIFU heating. This is because although the volume to be heated by HIFU can be designed to include all the potential sites of disease, the only places where the BBB will be selectively permeabilized are at the locations of the engineered stem cells which have migrated to the diseased sites. In contrast, previous methods that attempted to open the BBB with the physical disruptions caused by HIFU require precise knowledge of where the disease foci are located. If the locations of disease foci are unknown or only partially known with current imaging technologies or by other means, the volume of BBB permeabilization required to include all the potential sites of disease will be much larger than needed, which may lead to more potential side effects, in contrast to our approach that will only effectively open the BBB at the site of disease.

Mesenchymal stem cells (MSCs) have become valuable candidates for cell-based therapy for different CNS diseases including neurodegenerative disease and brain cancer and are compelling to be considered as vehicles for delivery of diagnostic and therapeutic agents[37]. The benefits of using MSCs clinically include easy accessibility and isolation from bone marrow as well as ease of in vitro expansion in cell culture[38]. MSCs have

demonstrated preferential incorporation into sites of tumor development and injury [33, 39]. Furthermore, MSCs have been genetically engineered for enhanced target homing and improved secretome, so that they can be more effectively targeted to sites of inflammation to achieve therapeutically relevant concentrations of biological agents [40–43]. TNFα is a multifunctional cytokine that plays a key role in apoptosis and cell survival as well as in inflammation and immunity[44]. Previous studies demonstrated that TNFα can act synergistically with cytostatic drugs and radiation for tumor therapy. Because it has been implicated in a wide spectrum of other diseases, the current use of TNFα in cancer is limited to regional administration for treatment of advanced soft tissue sarcomas and metastatic melanomas[45]. Several studies have demonstrated that TNFα activates and enhances BBB permeability [46–49]. Spatiotemporal control of TNFα expression in brain represents a promising way to focally permeabilize BBB while avoiding its systemic toxicity. The promoter for the heat shock protein 70 gene has been extensively used as a heat-inducible promoter to control therapeutic gene expression in tissues[25, 50]. The kinetics of heat shock protein induction and thermo-tolerance development has been well studied[50, 51]. We engineered MSCs using heat-inducible HSP70 expression system (Fig 1.). The gene expression activity driven by HSP70 promoter was found to be tissue specific and dependent on induction temperature and duration of induction time which are consistent with our observations (Fig. 1 and Supplentary Fig. 1).

High-intensity focused ultrasound (HIFU) has been used clinically to locally heat and ablate tissues. Focused ultrasound can concentrate acoustic energy to a focal spot of a few millimeters in diameter or larger sizes depending on the applications. Generally, a micro-bubble contrast agent needs to be systemically administered prior to ultrasound treatment for permeabilizing the BBB. The mechanical forces from oscillation of circulating bubbles driven by focused ultrasound change the array of endothelial cells in the blood vessel wall, thus transiently increasing the permeability of the BBB. MR-guided focused ultrasound has also been used to locally activate gene expression driven by HSP70 promoter in vivo. Furthermore, transcranial HIFU has been used in clinical trials to precisely heat or ablate targeted areas in the brain. In particular, there is already a commercially available clinical HIFU system (InSightec, Inc.) that is being used to transcranially treat various brain disorders including essential tremors, Parkinson’s disease and brain cancer. In the process described in this study HIFU is only used to heat local regions of the brain to around 43°C for gene activation (Fig. 2 and Fig. 4). Therefore, we are not constrained to only treating focal areas, a restriction that may limit the treating volume for reaching ablation temperatures (55°C). Heating tissues to around 43°C only requires a fraction of the energy needed for ablation and has been demonstrated to be possible over large volumes in preclinical and clinical settings. Since the mild heating that is required for our technology to work is much lower than that required for ablation the commercially available clinical HIFU system can be adapted quite easily for translating our technology into the clinic. It is noteworthy that the heat-inducible gene expression of engineered MSCs demonstrated good response to a relatively broad range of induction temperature from 42 to 44°C (Fig. 1). The good tolerance of gene expression to temperature variability will reduce the challenge of applying our technology in clinical practice and is beneficial for clinical translation of our technology. For the safety of our technology, 15–30 minutes heating dose at non-toxic

temperatures (42°C–44°C) used in our in vivo studies is the treatment parameter set optimized in our in-vitro studies to maximally activate the gene expression of several different cell lines including engineered MSC and Jurkat cells. The peak temperature and deposited thermal doses for gene induction are much lower than the safety thresholds to damage brain tissue. A previous study found that the thermal dose threshold for brain tissue damage was 48.0–50.8°C and 12.3–40.1 equivalent minutes [52]. Since the thermal dose used in our studies were much less than the published threshold dose for causing damage in brain tissue we do not expect any brain tissue damage in our study.

The Enhanced permeability and retention (EPR) effect is a major advantage of using nanoparticles for drug delivery. However, for EPR to work in the brain the BBB has to be permeable to the nanoparticles in the diseased tissues. Although some diseases are associated with increased permeability of the BBB but this is usually not uniform throughout the diseased tissues making it difficult to deliver nanoparticles to all diseased tissues. Our data showed that our approach can permeabilize the BBB for delivery of nanoparticles at least up to 300 nm in size (Fig. 4D). This demonstrates that our strategy is well designed to couple with the EPR effect of nanoparticle therapy by focally permeabilizing the BBB in the regions of the disease foci even when the disease itself does not cause increased BBB permeability to occur.

Though MSCs were intracranially injected into brain in this study, our long-term objective is to deliver the engineered stem cells into brain by systemic administration for BBB opening and for the treatment of brain diseases such as GBM. Systemic injected stem cells can sense the signals from GBM in the brain pass through BBB and migrate specifically to a brain tumor mass [53, 54]. Due to the existence of BBB, the low numbers of stem cells transmigrated into the brain across BBB may not be enough for a successful stem cell-based therapy. Our next step is to use HIFU to drive the production of a pro-inflammatory factor by the MSCs in the GBM tumor region, which will increase BBB permeability and further increase stem cell trafficking and accumulation at the tumor site. This process, the controlled amplification of stem-cell trafficking, may be repeated to serially amplify the effect, hopefully to the point at which the therapeutic payload carried by the stem cells achieves sufficient concentration to be effective.

In summary, we have developed a remote controlled cell-based therapeutic platform that offers unprecedented capabilities to (i) spatially and temporally control therapeutic expression; (ii) precisely and non-invasively permeabilize BBB; and (iii) leverage the EPR effect of nanotheranostics. This therapeutic platform can be modified to facilitate delivery of different diagnostic and therapeutic agents which can have great impact in treatment of GBM, other brain neoplasms and other disease processes in the central nervous system.

Supplementary Material

Refer to Web version on PubMed Central for supplementary material.

Acknowledgments

This work was supported by a grant of the National Cancer Institute (NCI) (R01 CA184091-01) and Wells Fargo Scholar Program. We thank Ms. Debra Fuller and Sandra Kaminsky for their technical support in MRI scan. We thank Ms. Dongqin Zhu for her technical support in transcranial surgery and stem cell implantation. We also thank Ms. Yue Huang for her technical support in cryosectioning of frozen brain tissue.

References

1. Abbott NJ, Ronnback L, Hansson E. Astrocyte-endothelial interactions at the blood-brain barrier. Nat Rev Neurosci. 2006; 7:41–53. [PubMed: 16371949]
2. Abbott NJ, Patabendige AAK, Dolman DEM, Yusof SR, Begley DJ. Structure and function of the blood-brain barrier. Neurobiol Dis. 2010; 37:13–25. [PubMed: 19664713]
3. Edwards RH. Drug delivery via the blood-brain barrier. Nat Neurosci. 2001; 4:221–222. [PubMed: 11224531]
4. Pardridge WM. The blood-brain barrier: bottleneck in brain drug development. NeuroRx. 2005; 2:3–14. [PubMed: 15717053]
5. Pollay M. Outwitting the blood-brain barrier for therapeutic purposes: Osmotic opening and other means - Comment. Neurosurgery. 1998; 42:1099–1099.
6. Neuwelt E, Abbott N, Abrey L, Banks WA, Blakley B, Davis T, Engelhardt B, Grammas P, Nedergaard M, Nutt J, Pardridge W, Rosenberg GA, Smith Q, Drewes LR. Strategies to advance translational research into brain barriers. Lancet Neurol. 2008; 7:84–96. [PubMed: 18093565]
7. Ulbrich K, Knobloch T, Kreuter J. Targeting the insulin receptor: nanoparticles for drug delivery across the blood–brain barrier (BBB). J Drug Target. 2011; 19:125–132. [PubMed: 20387992]
8. Rapoport SI, Robinson PJ. Tight-Junctional Modification as the Basis of Osmotic Opening of the Blood-Brain-Barrier. Ann NY Acad Sci. 1986; 481:250–267. [PubMed: 3468860]
9. Rapoport SI. Advances in osmotic opening of the blood-brain barrier to enhance CNS chemotherapy. Expert Opin Inv Drug. 2001; 10:1809–1818.
10. Bellavance MA, Blanchette M, Fortin D. Recent advances in blood-brain barrier disruption as a CNS delivery strategy. AAPS J. 2008; 10:166–177. [PubMed: 18446517]
11. Robertson DM, Raymond JJ, Dinsdale HB. Pharmacological Modification of Bradykinin Induced Breakdown of the Blood-Brain-Barrier. Can J Neurol Sci. 1987; 14:343–343.
12. Greenberg HS. Enhanced tumor uptake of carboplatin and survival in glioma-bearing rats by intracarotid infusion of bradykinin analog, RMP-7 - Comment. Neurosurgery. 1996; 39:133–133.
13. Prados MD, Schold SC, Fine HA, Jaeckle K, Hochberg F, Mechtler L, Fetell MR, Phuphanich S, Feun L, Janus TJ, Ford K, Graney W. A randomized, double-blind, placebo-controlled, phase 2 study of RMP-7 in combination with carboplatin administered intravenously for the treatment of recurrent malignant glioma. Neuro Oncol. 2003; 5:96–103. [PubMed: 12672281]
14. Carman AJ, Mills JH, Krenz A, Kim DG, Bynoe MS. Adenosine Receptor Signaling Modulates Permeability of the Blood-Brain Barrier. J Neurosci. 2011; 31:13272–13280. [PubMed: 21917810]
15. O'Reilly MA, Waspe AC, Chopra R, Hynynen K. MRI-guided disruption of the blood-brain barrier using transcranial focused ultrasound in a rat model. J Vis Exp. 2012
16. Dromi S, Frenkel V, Luk A, Traughber B, Angstadt M, Bur M, Poff J, Xie J, Libutti SK, Li KC, Wood BJ. Pulsed-high intensity focused ultrasound and low temperature-sensitive liposomes for enhanced targeted drug delivery and antitumor effect. Clin Cancer Res. 2007; 13:2722–2727. [PubMed: 17473205]
17. Etame AB, Diaz RJ, Smith CA, Mainprize TG, Hynynen K, Rutka JT. Focused ultrasound disruption of the blood-brain barrier: a new frontier for therapeutic delivery in molecular neurooncology. Neurosurg Focus. 2012; 32:E3. [PubMed: 22208896]
18. O'Reilly MA, Hynynen K. Ultrasound enhanced drug delivery to the brain and central nervous system. Int J Hyperthermia. 2012; 28:386–396. [PubMed: 22621739]
19. Hynynen K. Ultrasound for drug and gene delivery to the brain. Adv Drug Deliv Rev. 2008; 60:1209–1217. [PubMed: 18486271]

20. Sozio P, Cerasa LS, Abbadessa A, Di Stefano A. Designing prodrugs for the treatment of Parkinson's disease. Expert Opin Drug Dis. 2012; 7:385–406.
21. Wong HL, Wu XY, Bendayan R. Nanotechnological advances for the delivery of CNS therapeutics. Adv Drug Deliver Rev. 2012; 64:686–700.
22. Stanley SA, Sauer J, Kane RS, Dordick JS, Friedman JM. Remote regulation of glucose homeostasis in mice using genetically encoded nanoparticles. Nat Med. 2015; 21:92–98. [PubMed: 25501906]
23. Polstein LR, Gersbach CA. Light-Inducible Spatiotemporal Control of Gene Activation by Customizable Zinc Finger Transcription Factors. J Am Chem Soc. 2012; 134:16480–16483. [PubMed: 22963237]
24. Konermann S, Brigham MD, Trevino AE, Hsu PD, Heidenreich M, Cong L, Platt RJ, Scott DA, Church GM, Zhang F. Optical control of mammalian endogenous transcription and epigenetic states. Nature. 2013; 500:472–476. [PubMed: 23877069]
25. Eker OF, Quesson B, Rome C, Arsaut J, Deminiere C, Moonen CT, Grenier N, Couillaud F. Combination of Cell Delivery and Thermoinducible Transcription for in Vivo Spatiotemporal Control of Gene Expression: A Feasibility Study. Radiology. 2011; 258:496–504. [PubMed: 21163917]
26. Deckers R, Quesson B, Arsaut J, Eimer S, Couillaud F, Moonen CTW. Image-guided, noninvasive, spatiotemporal control of gene expression. P Natl Acad Sci USA. 2009; 106:1175–1180.
27. Rome C, Couillaud F, Moonen CTW. Spatial and temporal control of expression of therapeutic genes using heat shock protein promoters. Methods. 2005; 35:188–198. [PubMed: 15649846]
28. Ram Z, Cohen ZR, Harnof S, Tal S, Faibel M, Nass D, Maier SE. Magnetic resonance imaging-guided, high-intensity focused ultrasound for brain tumor therapy. Neurosurgery. 2006; 59:949–955. [PubMed: 17143231]
29. Jolesz FA, McDannold NJ. Magnetic Resonance-Guided Focused Ultrasound A New Technology for Clinical Neurosciences. Neurol Clin. 2014; 32:253–69. [PubMed: 24287394]
30. Hynynen K, Sun J. Trans-skull ultrasound therapy: the feasibility of using image-derived skull thickness information to correct the phase distortion. IEEE Trans Ultrason Ferroelectr Freq Control. 1999; 46:752–755. [PubMed: 18238476]
31. Dwyer RM, Khan S, Barry FP, O'Brien T, Kerin MJ. Advances in mesenchymal stem cell-mediated gene therapy for cancer. Stem Cell Res Ther. 2010; 1
32. Robinton DA, Daley GQ. The promise of induced pluripotent stem cells in research and therapy. Nature. 2012; 481:295–305. [PubMed: 22258608]
33. Kidd S, Spaeth E, Dembinski JL, Dietrich M, Watson K, Klopp A, Battula VL, Weil M, Andreeff M, Marini FC. Direct Evidence of Mesenchymal Stem Cell Tropism for Tumor and Wounding Microenvironments Using In Vivo Bioluminescent Imaging. Stem Cells. 2009; 27:2614–2623. [PubMed: 19650040]
34. Kim SU, de Vellis J. Stem Cell-Based Cell Therapy in Neurological Diseases: A Review. J Neurosci Res. 2009; 87:2183–2200. [PubMed: 19301431]
35. Zhao WA, Phinney DG, Bonnet D, Dominici M, Krampera M. Mesenchymal Stem Cell Biodistribution, Migration, and Homing In Vivo. Stem Cells Int. 2014
36. Peters RD, Hinks RS, Henkelman RM. Ex vivo tissue-type independence in proton-resonance frequency shift MR thermometry. Magn Reson Med. 1998; 40:454–459. [PubMed: 9727949]
37. Shah K. Mesenchymal stem cells engineered for cancer therapy. Adv Drug Deliver Rev. 2012; 64:739–748.
38. Malgieri A, Kantzari E, Patrizi MP, Gambardella S. Bone marrow and umbilical cord blood human mesenchymal stem cells: state of the art. Int J Clin Exp Med. 2010; 3:248–269. [PubMed: 21072260]
39. Karp JM, Teol GSL. Mesenchymal Stem Cell Homing: The Devil Is in the Details. Cell Stem Cell. 2009; 4:206–216. [PubMed: 19265660]
40. Ankrum J, Karp JM. Mesenchymal stem cell therapy: Two steps forward, one step back. Trends Mol Med. 2010; 16:203–209. [PubMed: 20335067]
41. Levy O, Zhao WA, Mortensen LJ, LeBlanc S, Tsang K, Fu MY, Phillips JA, Sagar V, Anandakumaran P, Ngai J, Cui CH, Eimon P, Angel M, Lin CP, Yanik MF, Karp JM. mRNA-

engineered mesenchymal stem cells for targeted delivery of interleukin-10 to sites of inflammation. Blood. 2013; 122:E23–E32. [PubMed: 23980067]

42. Kang SK, Shin IS, Ko MS, Jo JY, Ra JC. Journey of Mesenchymal Stem Cells for Homing: Strategies to Enhance Efficacy and Safety of Stem Cell Therapy. Stem Cells Int. 2012
43. Naderi-Meshkin H, Bahrami AR, Bidkhori HR, Mirahmadi M, Ahmadiankia N. Strategies to improve homing of mesenchymal stem cells for greater efficacy in stem cell therapy. Cell Biol Int. 2015; 39:23–34. [PubMed: 25231104]
44. Balkwill F. Tumour necrosis factor and cancer. Nature reviews Cancer. 2009; 9:361–371. [PubMed: 19343034]
45. Lejeune FJ. High dose recombinant tumour necrosis factor (rTNF alpha) administered by isolation perfusion for advanced tumours of the limbs: a model for biochemotherapy of cancer. Euro J Cancer. 1995; 31A:1009–1016.
46. Seki T, Carroll F, Illingworth S, Green N, Cawood R, Bachtarzi H, Subr V, Fisher KD, Seymour LW. Tumour necrosis factor-alpha increases extravasation of virus particles into tumour tissue by activating the Rho A/Rho kinase pathway. J Control Release. 2011; 156:381–389. [PubMed: 21884739]
47. Yang GY, Gong C, Qin Z, Liu XH, Lorris Betz A. Tumor necrosis factor alpha expression produces increased blood-brain barrier permeability following temporary focal cerebral ischemia in mice. Brain Res Mol Brain Res. 1999; 69:135–143. [PubMed: 10350645]
48. Connell JJ, Chatain G, Cornelissen B, Vallis KA, Hamilton A, Seymour L, Anthony DC, Sibson NR. Selective permeabilization of the blood-brain barrier at sites of metastasis. J Natl Cancer Inst. 2013; 105:1634–1643. [PubMed: 24108809]
49. Tsao N, Hsu HP, Wu CM, Liu CC, Lei HY. Tumour necrosis factor-alpha causes an increase in blood-brain barrier permeability during sepsis. J Med Microbiol. 2001; 50:812–821. [PubMed: 11549183]
50. Hundt W, Schink C, Steinbach S, O'Connell-Rodwell CE, Mayer D, Burbelko M, Kiessling A, Guccione S. Use of in vivo bioluminescence and MRI to determine hyperthermia-induced changes in luciferase activity under the control of an hsp70 promoter. NMR Biomed. 2012; 25:1378–1391. [PubMed: 22566294]
51. Diller KR. Stress protein expression kinetics. Annu Rev Biomed Eng. 2006; 8:403–424. [PubMed: 16834562]
52. McDannold N, Vykhodtseva N, Jolesz FA, Hynynen K. MRI investigation of the threshold for thermally induced blood–brain barrier disruption and brain tissue damage in the rabbit brain. Magnetic Resonance in Medicine. 2004; 51:913–923. [PubMed: 15122673]
53. Diaz-Coranguez M, Segovia J, Lopez-Ornelas A, Puerta-Guardo H, Ludert J, Chavez B, Meraz-Cruz N, Gonzalez-Mariscal L. Transmigration of Neural Stem Cells across the Blood Brain Barrier Induced by Glioma Cells. PloS One. 2013; 8:e60655. [PubMed: 23637756]
54. Aboody KS, Brown A, Rainov NG, Bower KA, Liu S, Yang W, Small JE, Herrlinger U, Ourednik V, Black PM, Breakefield XO, Snyder EY. Neural stem cells display extensive tropism for pathology in adult brain: evidence from intracranial gliomas. Proc Natl Acad Sci USA. 2000; 97:12846–12851. [PubMed: 11070094]

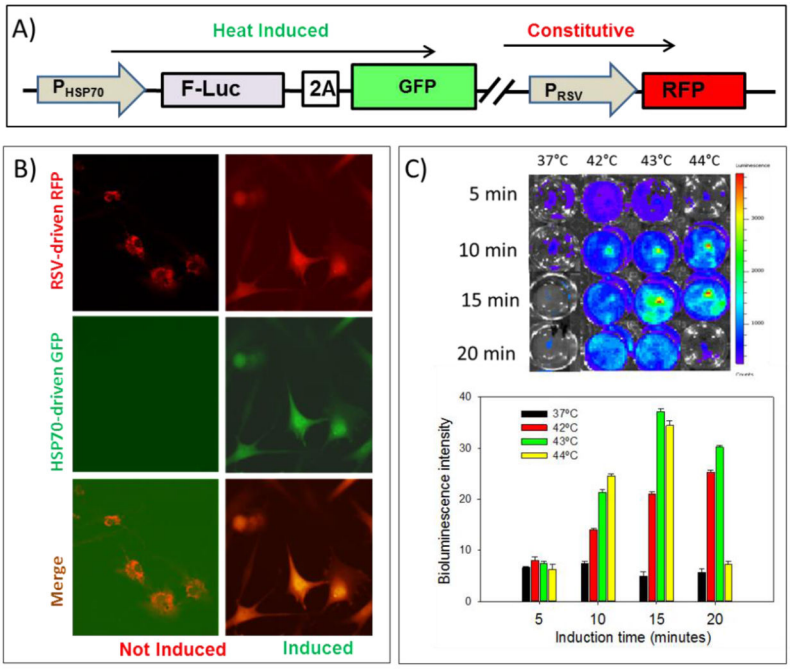

Fig. 1.

In vitro validation of heat-induced gene expression in MSCs cells. **A**) Schematic representation of the heat-inducible lentiviral plasmid construct pLenti-HSP70(F-Luc-2A-GFP)-RSV(RFP-BSD). **B**) HSP70-driven GFP expression by MSCs after exposure to 43°C for 15 minutes. Red: RFP fluorescence (545nm/620nm, Ex/Em); Green: GFP fluorescence (475nm/510–525nm, Ex/Em). **C**) Representative bioluminescence images and luciferase activity of MSCs-HSP70(F-Luc-2A-GFP) after exposure to different induction times and different temperatures.

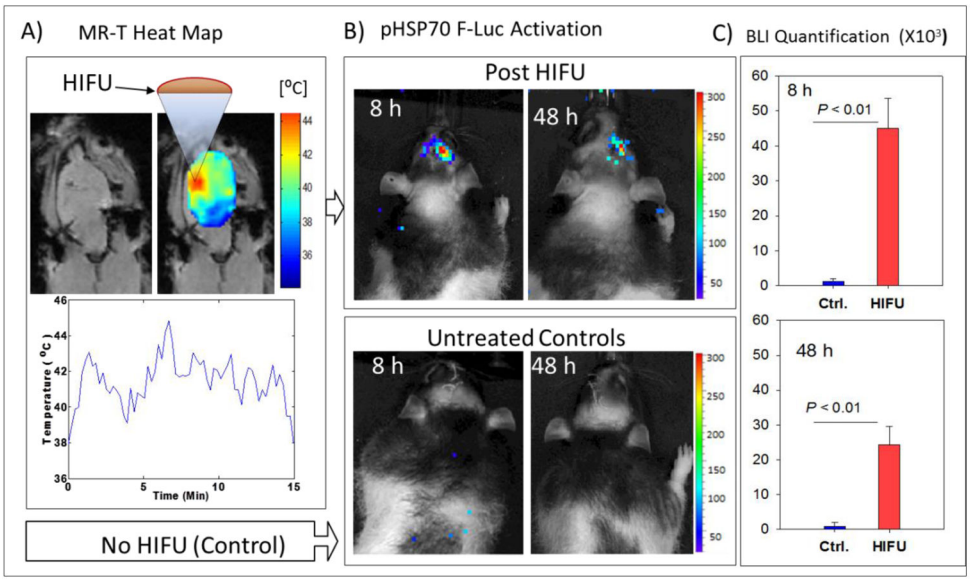

Fig. 2.

MRI-guided HIFU-induced transgene expression of engineered MSCs in rat brain. A) MRI T2-weighted image of the rat brain (upper left panel), MRI temperature map (color-coded) superimposed on the anatomical MRI image (upper right panel), and a typical time course of the temperature evolution during HIFU induction (lower panel). B) HSP70 driven reporter expression after HIFU treatment by bioluminescence imaging. C) Quantitation of BLI signal. Region of interest (ROI) were drawn over the brain sites and photon flux was quantitated and graphed at 8 and 48 hours after HIFU treatment.

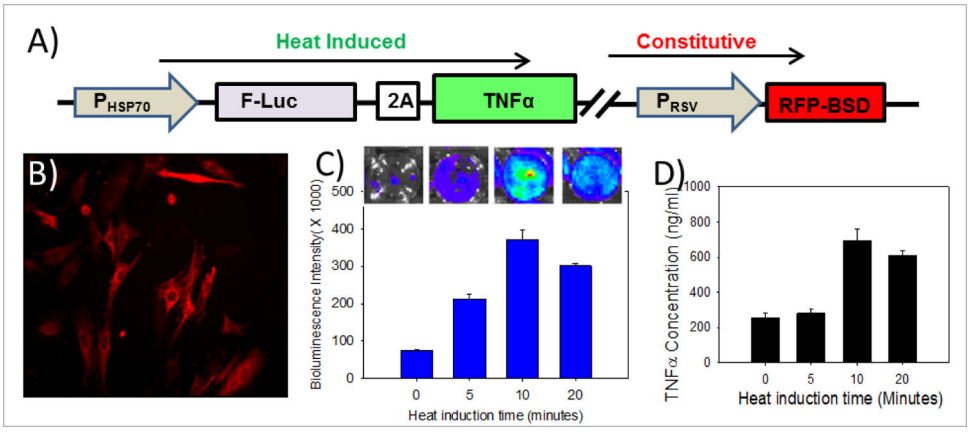

Fig. 3.

Heat-induced gene expressions by MSCs engineered with HSP70-driven F-Luc and TNFα genes. A) Schematic representation of the heat-inducible lentiviral plasmid construct pLenti-HSP70(F-Luc-2A-TNFα)-RSV(RFP-BSD). B) Representative fluorescent images of MSCs transduced with pLenti-HSP70(TNFα-Luc). C) Heat-activated luciferase expression of MSCs-HSP70(F-Luc-2A-TNFα). D) Heat-induced TNFα expression of MSCs-HSP70(F-Luc-2A-TNFα).

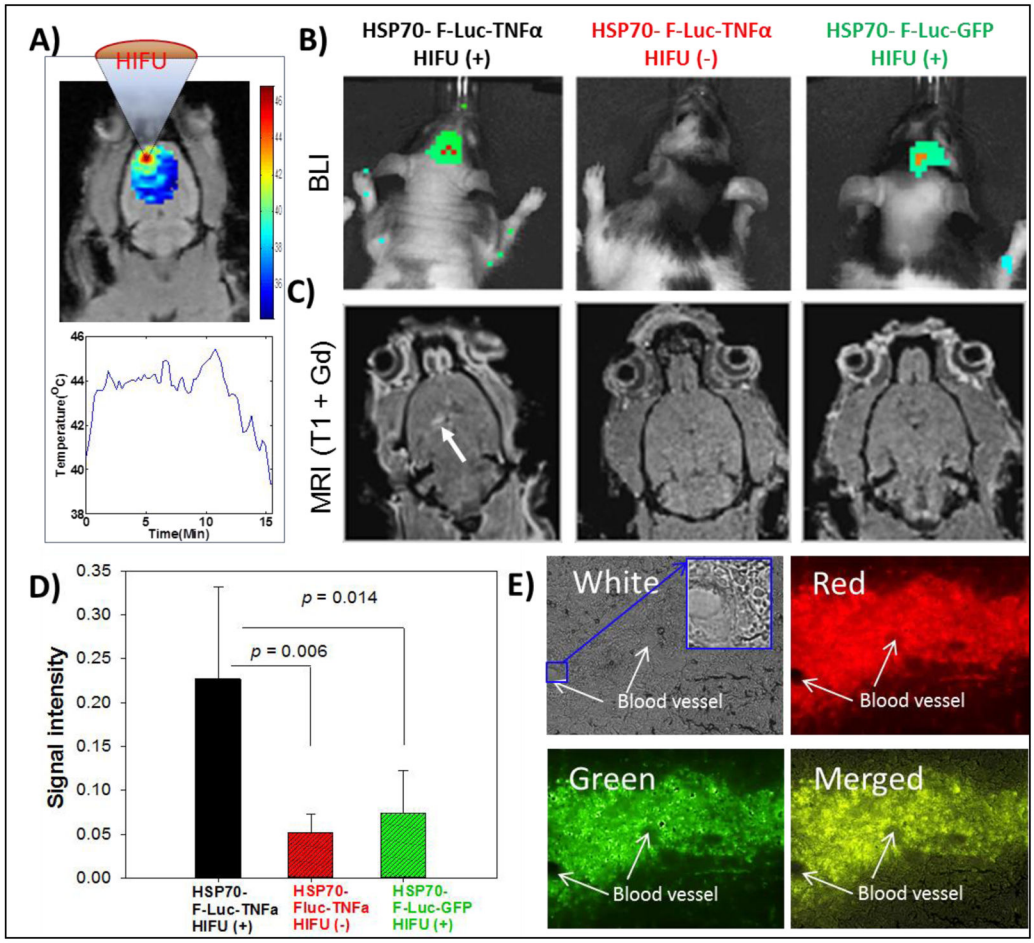

Fig. 4.

MRI-guided HIFU activation of TNFα production by MSCs to permeabilize BBB. MSCs-HSP70(F-Luc-2A-TNFα) or MSCs-HSP70(F-Luc-2A-GFP) were stereotactically implanted into the brains of athymic nude rats (1×10^6 cells per rat). A) Temperature map of the injection area when heated by HIFU under guidance of MRI to induce TNFα expression 3 days after cell implantation. B) The luciferase expression by bioluminescence after luciferin injection 1 day after HIFU induction. C) T1-weighted MRI images after intravenous injection of the MRI contrast agent (Magnevist, 0.125 mmol/kg) by tail vein 2 days after HIFU induction. D) Quantification of the signal intensity of T1-enhanced contrast in the region of interest in the brains of rats after systemic injection of MR contrast agent. E) BBB opening for nanoparticle penetration. Red: red fluorescence-labeled PLGA nanoparticles. Green: green fluorescence labeled PLGA nanoparticles. The brain blood vessels were indicated by white arrows.